ACS APPLIED MATERIALS & INTERFACES

Research Article

www.acsami.org

Fuel-Assisted Solution Route to Nanostructured Nickel Oxide Films for Electrochromic Device Application

Kun-Keng Chiang and Jih-Jen Wu*

Department of Chemical Engineering, National Cheng Kung University, Tainan 701, Taiwan

Supporting Information

ABSTRACT: In this work, nanocrystalline NiO films were prepared using the fuel-assisted solution method. The microstructure of the NiO film can be modulated by the addition of thiourea fuel. The size of NiO nanocrystals in the NiO film decreased with increasing amount of thiourea in the precursor solution. Compared to the film prepared without thiourea addition, the thiourea-assisted NiO film had enhanced electrochromic properties, including larger transmittance modulation, larger coloration efficiency, faster response time, and superior reliability. Electrochemical impedance spectroscopy measurements indicate that faster charge transfer occurs at the interface between the electrolyte and the fuel-assisted NiO films, which results in improved electrochromic behavior.

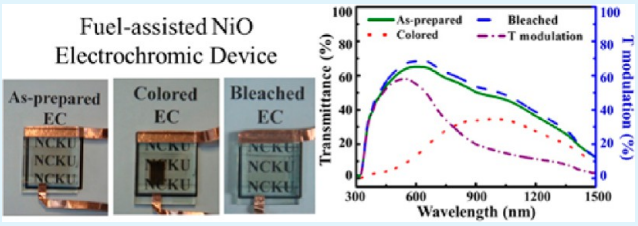

KEYWORDS: *nickel oxide film, fuel-assisted solution method,nanostructure, electrochromic device, electrochemical impedance spectroscopy, charge transfer*

INTRODUCTION

Due to their reversible transmittance in response to an applied voltage,[1−3] electrochromic (EC) materials have drawn considerable attention for application in smart windows[4] and information displays.[1] Electrochromism occurs in a number of organic and inorganic materials.[2] Among them, nickel oxide is a promising anodic EC material with high EC efficiency, large dynamic range, good cyclic reversibility, and low material cost.[1,5] Electrochromic NiO films have been deposited via many techniques, such as sputtering,[6,7] laser ablation,[8,9] vaporation,[10] sol−gel,[11] spray pyrolysis,[12] and electrodeposition.[13] NiO can be changed from a transparent state to a colored one by the insertion of OH^- ions with charge-balancing electrons extracted from the valence band at the same time.[1] The electrochemical reaction of insertion/extraction involves a charge transfer reaction at the interface between NiO and the electrolyte as well as diffusion of OH^- ions within the NiO structure. It has been reported that slow switching speed and low color contrast, which depend on the microstructure of the film, are the main issues in current NiO EC films.[14] The response times of coloration and bleaching are related to the charge transfer rate at the EC material/electrolyte interface, the diffusion coefficient of the ions within the EC material, and the diffusion distance to the active sites. Therefore, an appropriate design of the microstructure of the EC material is crucial for its EC properties.

The fuel-assisted solution method, which is conducted by using an appropriate pair of fuel and oxidizer in the precursor solution, has been demonstrated to be an efficient chemical route for preparing nanostructured metal oxide film.[15−18] Due to the exothermic reaction ignited by fuel during process, the formation temperature of the crystalline oxide film can therefore be reduced significantly.[15] Moreover, the microstructure of the film can be easily altered by the amount of fuel added in the precursor solution.[16−18] We have previously demonstrated the formation of tungsten oxide films using a thiourea (fuel)-assisted solution process and their application to EC devices and resistive random access memory (RRAM).[16,17] Recently, we further investigated the deposition of glycine-assisted nickel oxide films on indium tin oxide (ITO) substrates and the resistive switching behaviors of Al/fuel-assisted NiO_x/ITO devices.[18] In this work, nanocrystalline NiO films were prepared using the thiourea-assisted method. The size of NiO nanocrystals in the NiO film can be decreased by increasing the amount of thiourea in the precursor solution. Compared to film prepared without thiourea addition, the thiourea-assisted NiO film has larger transmittance modulation and coloration efficiency (CE) with a fast response time and acceptable reliability. Electrochemical impedance spectroscopy (EIS) was employed to investigate the charge transfer and transport properties in the thiourea-assisted NiO films.

EXPERIMENTAL SECTION

Nickel nitrite (8 mmol, 99%, Merk) was dissolved into a mixture of 1 mL of hydrogen peroxide (30%, Sigma-Aldrich) and 9 mL of deionized water. Thiourea (99%, Sigma) was then added into the solution. The solution was stirred to evaporate the solvent until the weights of the solutions were 10 g. The precursor was spun onto a fluorine-doped tin oxide (FTO)-coated glass (Solarnix, sheet resistance: 8 $\Omega \cdot sq^{-1}$) substrate followed by annealing at 450 °C for 3 h with ramping rates of 32.5 $°C \cdot min^{-1}$ from room temperature to

Received: January 16, 2013
Accepted: June 24, 2013
Published: June 24, 2013

350 and 10 °C·min^{-1} to 400 °C. For simplicity, the films prepared using the precursor solutions with molar ratios of nickel nitrite to thiourea of 8:0, 8:2, and 8:3 were coded as 80-450T, 82-450T, and 83-450T films, respectively. The morphology and crystal structure of the nickel oxide films were examined using field-emission scanning electron microscopy (FESEM) as well as X-ray diffraction (XRD) and field-emission transmission electron microscopy (FETEM), respectively. The detailed information for these characterizations has been reported in the previous work.[18] The EC performances of the NiO films, including transmittance modulation, CE, and response times, were measured using EC devices.[16,19] A schematic of the NiO EC device is shown in Figure S1 (Supporting Information). The electrolyte solution of 1 M NaOH (Siagma-Aldrich) was employed in this work. The details for the EC device fabrication as well as transmittance modulation, CE, EC response time, cyclic voltammetry, and EIS measurements have been described elsewhere.[16−19]

RESULTS AND DISCUSSION

Figure 1 shows SEM images of the three nickel oxide films formed on FTO substrates using precursors with various molar ratios of nickel nitrate to thiourea. Figure 1a shows that a granular film formed on the FTO substrate in the absence of thiourea after being annealed at 450 °C (80-450T). Cracks appeared on the film formed using the precursor with a nickel nitrate to thiourea molar ratio of 8:2 (82-450T), as shown in Figure 1b. When the thiourea in the precursor was increased to a molar ratio of nickel nitrate to thiourea of 8:3 (83-450T), a rather smooth film formed on the FTO substrate, as shown in Figure 1c. The thicknesses of the three films are ∼200 nm, as shown in the cross-sectional SEM images in the insets of the figures.

Structural characterization of the three nickel oxide films was performed using glancing angle X-ray diffraction (GAXRD) and TEM. Figure 2 shows the GAXRD patterns of the three nickel oxide films on FTO substrates as well as the bare FTO substrate. In addition to the diffraction peaks pertaining to the FTO substrate, the other peaks in the GAXRD patterns can be indexed as those corresponding to cubic nickel oxide (ICDD-PDF no. 01-073-1519), indicating the formation of crystalline nickel oxide in the three films after annealing at 450 °C. It is worth noting that crystalline nickel sulfate hydrate existed in the thiourea-assisted films when the annealing temperature was below 450 °C, as revealed in the GAXRD patterns of Figure S2 (Supporting Information). The crystal sizes (d) in the three NiO films annealed at 450 °C were estimated using line broadenings of (200) diffraction peaks (widths at half-maximum intensity (β)) in the three XRD patterns with the Scherrer equation.[21]

$$d = K\lambda/\beta \cos\theta \quad (1)$$

where λ is the wavelength, θ is the diffraction angle, and K is a constant (chosen as 0.9). The crystal sizes for the 80−450T, 82−450T, and 83−450T films were calculated to be 18, 11.4, and 9.9 nm, respectively, showing that the crystal size decreases with increasing amount of thiourea in the precursor solution.

Cross-sectional TEM bright-field (BF) images of the 80-450T, 82-450T, and 83-450T films are shown in Figure 3a−c, respectively. The corresponding selected area electron diffraction (SAED) patterns of the NiO films are shown in Figure 3a−c. They reveal that cubic NiO nanocrystals existed in the thiourea-assisted films. Figure 3d−f displays the corresponding dark-field (DF) images of Figure 3a−c. The DF images confirm the XRD result that the size of NiO nanocrystals in the 80-450T film is significantly larger than

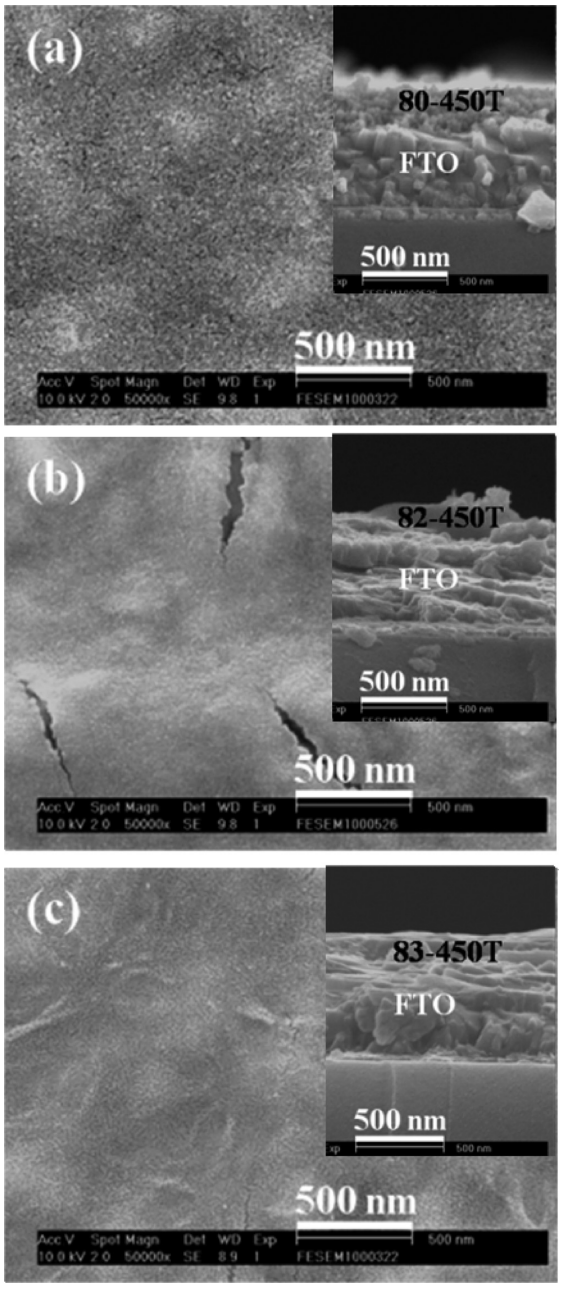

Figure 1. Top-view SEM images of three nickel oxide films formed on FTO substrates. (a) 80-450T, (b) 82-450T, and (c) 83-450T. The insets show the corresponding cross-sectional SEM images.

those in the 82-450T and 83-450T films. The HR TEM images of the 80-450T, 82-450T, and 83-450T films are shown in Figure 3g−i, respectively. The lattice spacings of 0.208 and 0.24 nm in the HRTEM images correspond to the d-spacings of (200) and (111) crystal planes of cubic NiO, respectively.

Figure 4 shows the transmittance spectra of the as-prepared, colored, and bleached states of the three NiO films. Photographs of the devices with the three different states are also shown in the figure. With the contribution of FTO substrates, the as-prepared 80-450T film has ∼70% transmittance whereas the transmittances of as-prepared 82-450T and 83-450T films are ∼65% at around 550 nm. The as-prepared device with the 80-450T film has higher transparence than those of the other two devices, as confirmed by the photographs in the as-prepared EC panels in Figure 4. After the

dx.doi.org/10.1021/am400192s | ACS Appl. Mater. Interfaces 2013, 5, 6502−6507

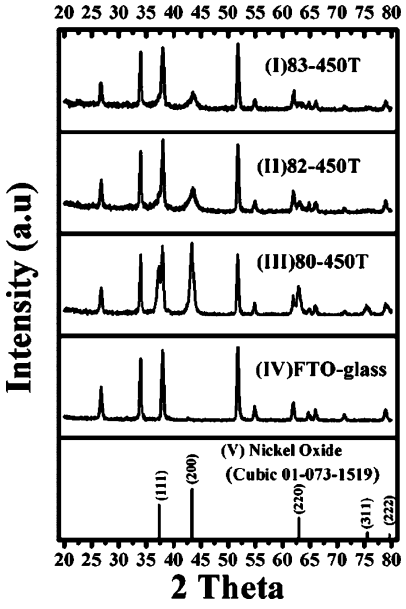

Figure 2. GAXRD patterns of nickel oxide films on FTO substrates and bare FTO substrate.

extraction of 40 mC·cm^{-2} electrons, as shown in Figure 4a, the transmittance of the 80-450T film at 550 nm is ∼65% and the device still looks transparent. In contrast, the transmittances of the thiourea-assisted 82-450T and 83-450T films in the wavelength range of 300−600 nm are less than 20% and 10%, respectively, as shown in Figure 4b and c. This indicates that the coloration behavior of the NiO film depends on the molar ratio of nickel nitrate to thiourea in the precursor solution. For a given number of extracted electrons, the transmittance of NiO film decreased with increasing thiourea in the precursor solution. The colored 83-450T device has a dark-brown color, as illustrated in the colored EC panel of Figure 4c.

The absorption spectra of the devices in the bleached state after the injection of 40 mC·cm^{-2} electrons are also shown in Figure 4. The spectra of the three bleached devices are similar, with the transmittances at 600 nm being ∼70%. The transmittances of the bleached 82-450T and 83-450T films are larger than those of their corresponding as-prepared films. Quite transparent devices were obtained, as shown in the bleached EC panels of Figure 4. The transmittance modulations of the three devices are shown in Figure 4 for comparison. The 80-450T film has a transmittance modulation of less than 10% in the whole wavelength region, as shown in Figure 4a. Significant transmittance modulations in the visible range were found in the thiourea-assisted 82-450T and 83-450T devices. The 83-450T film has the largest transmittance modulation (∼60% at 550 nm) among the three NiO films.

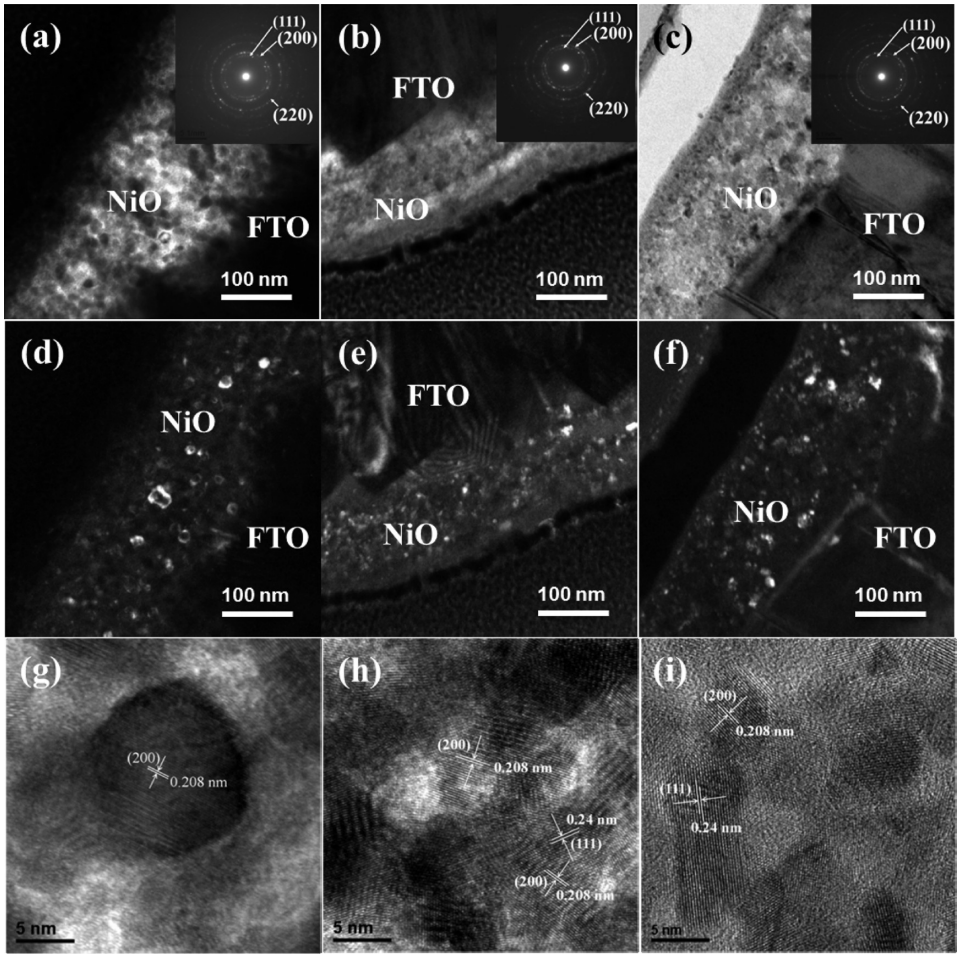

Figure 3. Cross-sectional BF images, corresponding SAED patterns (inset), DF images, and HR TEM images of (a, d, g) 80-450T, (b, e, h) 82-450T, and (c, f, i) 83-450T.

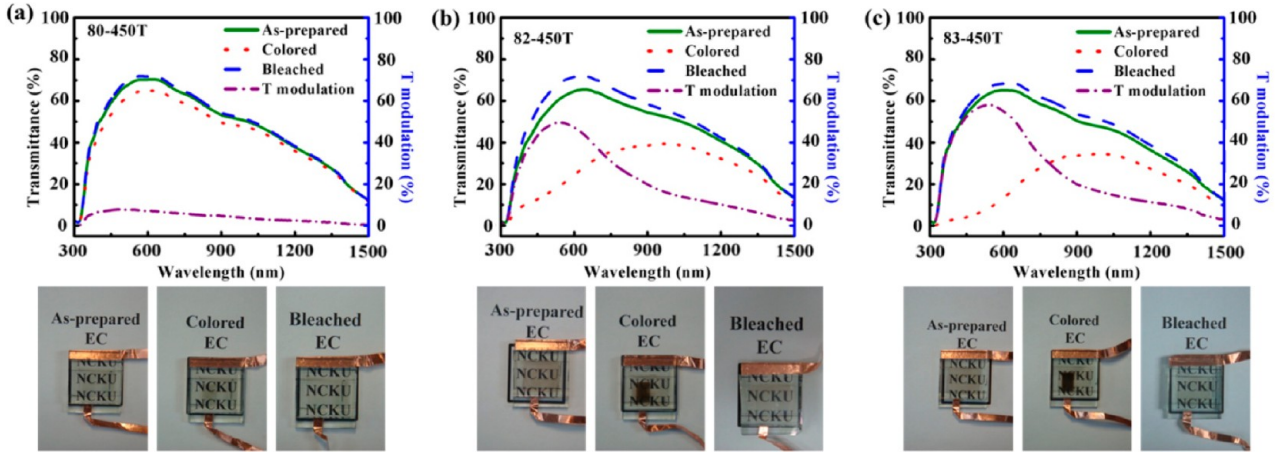

Figure 4. Transmittance spectra and corresponding photographs of as-prepared, colored, and bleached states of (a) 80-450T, (b) 82-450T, and (c) 83-450T.

Figure 5a shows the optical densities at 550 nm as a function of charge density of the three NiO films during the extraction of electrons at a constant current density of 50 $\mu A \cdot cm^{-2}$. The CE was calculated from the slopes of the curves in Figure 5a. The CEs of 80-450T, 82-450T, and 83-450T films are 12, 21.8, and 25.6 $cm^2 \cdot C^{-1}$, respectively. The thiourea-assisted NiO films have significantly higher CEs than that of the 80-450T NiO film. Comparing the two thiourea-assisted NiO films, the CE increased with thiourea concentration in the precursor solution. In addition, for a given thickness, the optical density of the 80-450T film became saturated at 0.2 after extraction at a charge density of 5 $mC \cdot cm^{-2}$. The saturated optical densities of the 82-450T and 83-450T films significantly increased to 0.7 and 1.0 after extraction at charge densities of 30 and 40 $mC \cdot cm^{-2}$, respectively, as shown in Figure 5a. The results indicate that the 83-450T film had the highest CE and largest saturated optical density among the three films.

The coloration and bleaching times of the three NiO films were measured using two-electrode EC devices with the application voltages of +2 and −2 V, respectively. Figure 5b shows the changes in the transmittances of the NiO films at 550 nm. With applied voltages of ±2 V, the transmittance modulations of the 80-450T, 82-450T, and 83-450T devices were ∼20%, ∼50%, and ∼60%, respectively. The coloration/bleaching times of the 82-450T and 83-450T devices are 11.3 s/6.7 s and 11.8 s/4 s, respectively, where the times are those required for a 40% change in transmittance.[16,19] The transmittance modulation of the 80−450T device was lower than 40%, and thus, the coloration and bleaching times could not be calculated.

The cyclic voltammograms (CVs) of the 83-450T film, which were obtained in the range of +0.7 to −0.5 V vs Ag/AgCl electrode, were measured to examine reliability for use in EC devices. As shown in Figure 5c, the anodic and cathodic peaks in the CV curves shift toward more positive and negative values, respectively, from the 10th to the 500th cycle. After the 500th cycle, the CV curves remain almost unchanged up to 1000 cycles. The total charge densities intercalated into the film at the 10th, 100th, 500th, 700th, and 1000th cycles are −24, −25.4, −23, −21.6, and −20.9 $mC \cdot cm^{-2}$, respectively, indicating excellent reliability.

The charge transfer/transport properties of the three NiO electrohromic devices were investigated using EIS. Figure 6 shows the EIS spectra of the three devices during coloration with an applied direct current (DC) voltage of 0.5 V. The equivalent circuit model of the EC electrode is illustrated in the inset of Figure 6a. Figure 6a shows the EIS spectrum of the 80-450T film, which is composed of a semicircle at high frequencies and a straight line at low frequencies. The fitting result based on the equivalent circuit model is also shown in the figure. The semicircle is ascribed to the impedance of the parallel combination of the charge-transfer resistance (R_{ct}) and the double-layer distributed constant phase element (CPE), and the straight line is associated with the complex impendence (Z_w) representing the diffusion of OH^- ions within the film.[16,19,20] This indicates that the kinetics of the OH^- ions intercalated into the 80-450T film is limited by diffusion at low frequencies. With increasing frequency, charge transfer at the interface becomes the rate-determining step of the intercalation process. The semicircle is absent in the EIS spectra of fuel-assisted NiO films (82-450T and 83-450T), as shown in Figure 6b and c, respectively. A straight line covers most of the frequency range in the EIS spectrum of the 83-450T film. The coloration mechanism comprises charge transfer at the interface between the electrolyte and electrode followed by charge diffusion in the EC film. The absence of the semicircle in the high-frequency range in the EIS spectra indicates that the charge transfer rates at the interface between the electrolyte and the thiourea-assisted NiO electrodes are too fast to be measured using the EIS technique (maximum frequency = 5×10^4 Hz). The EIS results therefore show that the kinetics of OH^- intercalation into the fuel-assisted NiO films is limited almost entirely by the diffusion rate.[20] The fast charge transfer rate likely plays a crucial role in enhancing the EC properties of thiourea-assisted NiO films.

The thiourea-assisted NiO films outperform the 80-450T film in terms of transmittance modulation and coloration efficiency. These EC enhancements are associated with the modification of the microstructures in the NiO films. As shown in Figures 2 and 3, the crystal size of the NiO film can be modulated by the addition of thiourea during the processing. We have previously demonstrated that for thiourea-assisted WO_3 films,[16] the gaseous species released at high temperatures[22] suppress the aggregation of the unit blocks, resulting in the formation of porous films with superior EC performance. In the present work, much smaller crystals formed in the thiourea-assisted NiO films. This is also ascribed to the gaseous species released at high temperatures through the decomposition of

dx.doi.org/10.1021/am400192s | ACS Appl. Mater. Interfaces 2013, 5, 6502−6507

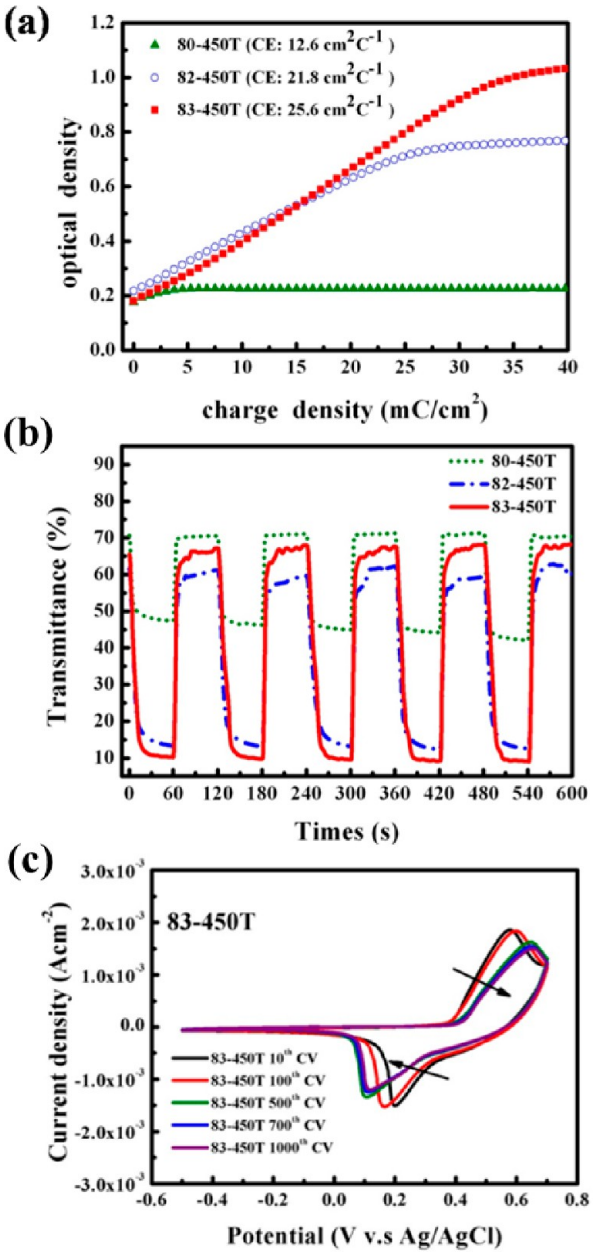

Figure 5. (a) In situ optical density vs charge density for NiO films during extration of electrons at a constant current density of 50 μA·cm^{-2}. (b) Changes in transmittance of NiO films at 550 nm with applied voltages of ±2 V. (c) CVs of 83-450T obtained in the range of +0.7 to −0.5 V vs Ag/AgCl electrode.

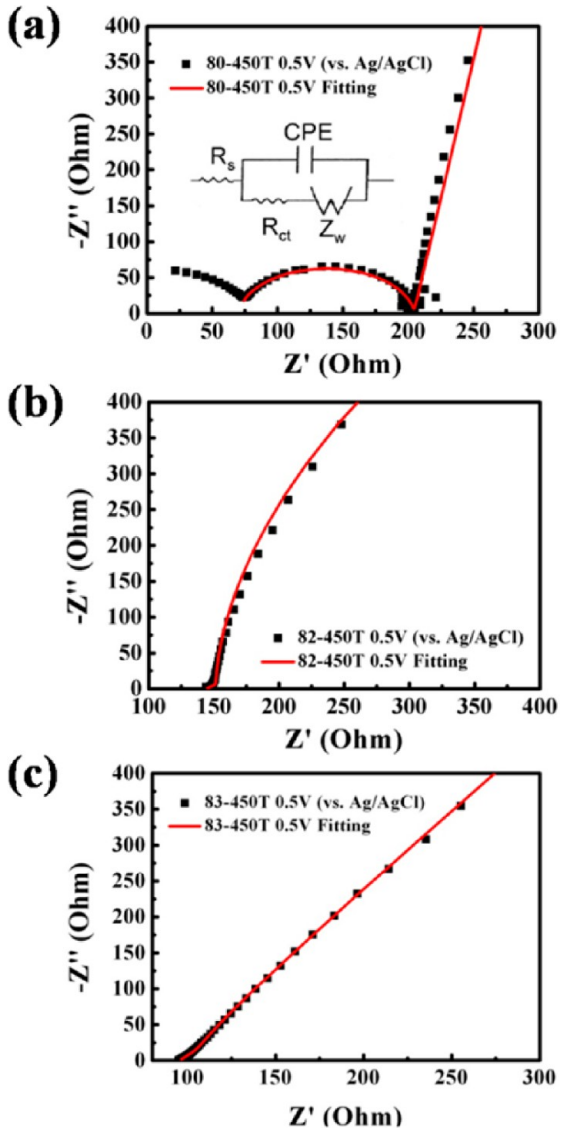

Figure 6. EIS spectra of three NiO devices during coloration with an applied DC voltage of 0.5 V vs Ag/AgCl electrode. The solid lines are the fitting results based on the equivalent circuit model shown in the inset of (a), where R_{ct} is the charge-transfer resistance, CPE is the double-layer distributed constant phase element, Z_w is the complex impedance representing the diffusion of OH^- ions within the film, and R_s is the uncompensated ohmic resistance of the electrolyte and electrode.

thiourea-related species in the precursor. The NiO unit blocks are surrounded by the gaseous species, which prevents aggregation at high temperatures.[23] The crystal size of the NiO film therefore decreases with increasing amount of thiourea in the precursor solution. Compared to the 80-450T film, the thiourea-assisted NiO film with smaller crystals, which provide a large surface area, facilitates charge transfer between the electrolyte and the NiO electrode. Therefore, the EC performance of the thiourea-assisted NiO films is superior to that of the film prepared without thiourea addition.

CONCLUSIONS

Nanocrystalline NiO films were prepared using the thiourea-assisted method. The microstructure of the NiO film can be modulated by the addition of thiourea fuel. The size of NiO nanocrystals in the NiO film decreased with increasing thiourea in the precursor solution. This is ascribed to the gaseous species released at high temperatures through the decomposition of thiourea-related species in the precursor. The NiO unit blocks are therefore surrounded by the gaseous species, which prevent aggregation at high temperatures. Compared to the film prepared without thiourea addition, the thiourea-assisted NiO film had improved EC properties; transmittance modulation increased from <10% to ~60%, and the coloration efficiency improved from 12 to 25.6 cm^2·C^{1-}. CVs indicate the excellent reliability of thiourea-assisted NiO film. The EIS results indicate that fast charge transfer occurs at the interface between the electrolyte and the thiourea-assisted NiO films. Thiourea-assisted NiO films with small crystals provide a large surface

area, facilitating the charge transfer between the electrolyte and the NiO electrode.

■ ASSOCIATED CONTENT

Supporting Information

Schematic of the NiO EC device and GAXRD patterns of the thiourea-assisted films annealed at temperatures lower than 450 °C. This material is available free of charge via the Internet at http://pubs.acs.org.

■ AUTHOR INFORMATION

Corresponding Author

*E-mail: wujj@mail.ncku.edu.tw.

Notes

The authors declare no competing financial interest.

■ ACKNOWLEDGMENTS

The authors gratefully acknowledge the financial support from the National Science Council of Taiwan (Grants NSC-101-3113-E-006-002 and NSC-100-2628-E-006-032-MY2).

■ REFERENCES

(1) Niklasson, G. A.; Granqvist, C. G. *J. Mater. Chem.* **2007**, *17*, 127−156.
(2) Monk, P. M. S.; Mortimer, R. J.; Rosseinsky, D. R. *Electrochromism: Fundamentals and Applications*; VCH: Weinheim, Germany, 1995.
(3) Granqvist,C. G. *Handbook of inorganic electrochromic materials*; Elsevier: The Netherlands, 2002.
(4) Hauch, A.; Georg, A.; Baumgartner, S.; Krasovec, U. O.; Orel, B. *Electrochim. Acta* **2001**, *46*, 2131−2136.
(5) Park, S. H.; Lim, J. W.; Yoo, S. J.; Cha, I. Y.; Sung, Y.-E. *Sol. Energy Mater. Sol. Cells* **2012**, *99*, 31−37.
(6) Ahn, K.-S.; Nah, Y.-C.; Park, J.-Y.; Sung, Y.-E.; Cho, K.-Y.; Shin, S.-S.; Park, J.-K. *Appl. Phys. Lett.* **2003**, *82*, 3379−3381.
(7) Magana, C. R.; Acosta, D. R.; Martinez, A. I.; Ortega, J. M. *Sol. Energy* **2006**, *80*, 161−169.
(8) Bouessay, I.; Rougier, A.; Tarascon, J.-M. *J. Electrochem. Soc.* **2004**, *151*, H145−H152.
(9) Penin, N.; Rougier, A.; Laffont, L.; Poizot, P.; Tarascon, J.-M. *Sol. Energy Mater. Sol. Cells* **2006**, *90*, 422−433.
(10) Verlevska, J.; Ristova, M. *Sol. Energy Mater. Sol. Cells* **2002**, *73*, 131−139.
(11) Jiao, Z.; Wu, M.-H.; Qin, Z.; Xu, H. *Nanotechnology* **2003**, *14*, 458−461.
(12) Kamal, H.; Elmaghraby, E. K.; Ali, S. A.; Abdel-Hady, K. *Thin Solid Films* **2005**, *483*, 330−339.
(13) Nakaoka, K.; Ueyama, J.; Ogura, K. *J. Electroanal. Chem.* **2004**, *571*, 93−99.
(14) Yuan, Y. F.; Xia, X. H.; Wu, J. B.; Chen, Y. B.; Yang, J. L.; Guo, S. Y. *Electrochim. Acta* **2011**, *56*, 1208−1212.
(15) Kim, M.-G.; Kanatzidis, M. G.; Facchetti, A.; Marks, T. J. *Nat. Mater.* **2011**, *10*, 382−388.
(16) Wu, W.-T.; Liao, W.-P.; Chen, J.-S.; Wu, J.-J. *ChemPhysChem* **2010**, *11*, 3306−3312.
(17) Wu, W.-T.; Wu, J.-J.; Chen, J.-S. *ACS Appl. Mater. Interfaces* **2011**, *3*, 2616−2621.
(18) Chiang, K.-K.; Chen, J.-S.; Wu, J.-J. *ACS Appl. Mater. Interfaces* **2012**, *4*, 4237−4245.
(19) Wu, W. T.; Liao, W. P.; Chen, L. Y.; Chen, J. S.; Wu, J. J. *Phys. Chem. Chem. Phys.* **2009**, *11*, 9751−9757.
(20) Ho, C.; Raistrick, I. D.; Huggins, R. A. *J. Electrochem. Soc.* **1980**, *127*, 343−350.
(21) Cullity, B. D.; Stock, S. R. *Elements of X-Ray Diffraction*, 3rd ed.; Prentice Hall: Upper Saddle River, NJ, 2001; p 170.
(22) Madarasz, J.; Pokol, G. *J. Therm. Anal. Calorim.* **2007**, *88*, 329−336.
(23) Wu, W.-T.; Chen, J.-S.; Wu, J.-J. *J. Am. Ceram. Soc.* **2010**, *93*, 2268−2273.